A tool for generating realistic noisy spike trains

Leslie S. Smith and Nhamoinesu Mtetwa [a]

[a] *Department of Computing Science and Mathematics, University of Stirling, UK*

Abstract

Spike detection and spike sorting techniques are often difficult to assess because of the lack of ground truth data (i.e. spike timings for each neuron). We present an analysis of the transmission of intracellular signals to an extracellular electrode, and a set of MATLAB functions which produce realistic noisy spike trains for which the ground truth is known. This can also be used to generate realistic (non Gaussian) background noise. The software is available on the web.

Key words: Spike detection, spike sorting, synthetic data.

1 Introduction

The primary aim of this tool is the generation of noisy spike trains to simulate the kind of signals that electrodes in extracellular multi-electrode arrays (MEAs) record in culture. The motivation for this tool is to provide "ground truth" data for the testing of algorithms for spike detection and spike sorting. For data acquired using MEAs, this information can only be available if there is concurrent intracellular recording of the neuron of interest: generally, this is simply impossible. The difficulty we are attempting to overcome is that without ground truth data, it is not possible to compare different spike detection and spike sorting techniques (the techniques are reviewed in Lewicki (1998)). This is a difficult problem: Wood et al. (2004) report over 20% errors using semiautomated spike sorting. Many authors have generated ground truth data by taking recordings which contain spikes, and mixing them and adding noise (e.g. Atiya, 1992; Chandra and Optican, 1997; Quiroga et al., 2004; Zhang et al., 2004), or re-generating data with similar statistics (Wood et al., 2004). This presumes that suitable data already exists, and that the form that noise should take is known. A different approach has been taken by Menne et al. (2002, 2005); Mamlouk et al. (2005): they used GENESIS (Bower and Beeman, 1998) to create a multi compartment simulation of relevant neural circuitry

(they are working in hippocampus), and then summed the contribution from each compartment assuming homogenous resistivity and no capacitance.

We are interested in generating signals that are useful for testing spike detection and sorting techniques for in vitro recordings, where the underlying neural structure (if any exists) is unknown. In general, all that is known is the approximate density of the neurons. Further, inspection of spike shapes suggests that there is indeed capacitance as well as resistance in the system. We have therefore taken a different approach, and attempted to analyse the signal transfer between the intracellular spike and the extracellular electrode in order to generate realistic test data for which the underlying spike patterns are known. A related approach was taken by Nakatani et al. (2001) in the context of cuff electrodes. For in vitro multi-electrode array (MEA) based recording, the culture is grown in dishes on which the electrodes are already present. Generally, the culture contains a mixture of neurons and glial cells, and there may be glial cells between the electrode and the neurons. Further, each electrode is usually near enough to a number of neurons to pick up signals from them. Unlike the situation in Menne's work, the electrodes are generally too far apart to pick up signals from the same neurons. Thus, ICA is not a usable option. The actual signal from each neuron is transformed by the effect of the path from spiking neuron to electrode. The details of this transformation are discussed in section 2. We have developed a set of MATLAB routines which allow the user to emulate this transformation for a number of neurons.

This paper is organised as follows: section 2 contains a theoretical discussion of the nature of the signal picked up by an electrode. This is followed by a discussion of the mechanism for generating signals which are like those from extracellular electrodes, and section 4 provides an example of a signal generated using the software. The software, and a user manual for it, are available (Smith and Mtetwa, 2005).

2 An analysis of cell recording

2.1 General formulation

We attempt to characterise the signal received at an extracellular electrode. Consider a current $I_{dA}(t)$ passing through a patch of membrane, dA at location $\vec{x}_i = \vec{x}_i(dA)$, where $\vec{x}_i$ is the vector from electrode i to the patch dA (see figure 1).

This will have an effect at electrode i, leading to a voltage $v_i(dA, t)$ being generated. Let us assume that the effect is linear in $I_A(t)$. If we characterise

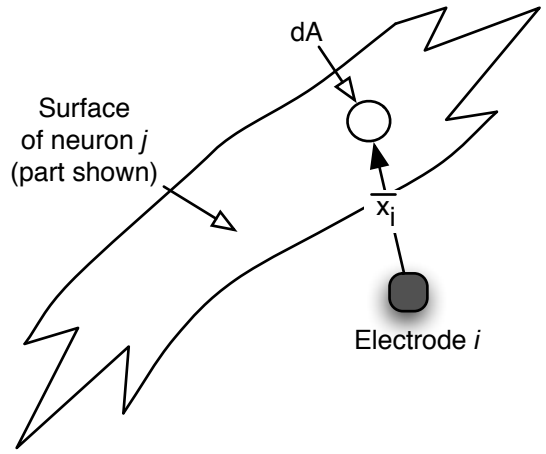

Figure 1. Electrode i and patch of membrane.

this effect by a response function $r(\vec{x_i})$ then the resultant potential at electrode i, will be

$$v_i(dA, t) = I_{dA}(t) r(\vec{x_i}(dA)) \tag{1}$$

We are assuming that the extracellular fluid is ohmic (see figure 2). Using linearity, we can consider the effect of the currents from a whole neuron j, with surface N_j,

$$v_i(N_j, t) = \int\limits_{dA \in N_j} I_{dA}(t) r(\vec{x_i}(dA)) dA \tag{2}$$

The total effect for all nearby neurons (indexed by j) is then

$$v_i(t) = \sum_j v_i(N_j, t) = \sum_j \int\limits_{dA \in N_j} I_{dA}(t) r(\vec{x_i}(dA)) dA \tag{3}$$

Note that $v_i(t)$ is the voltage arriving at the electrode i from the neurons: what actually gets recorded may differ. Some of the currents $I_{dA}(t)$ come from spikes (primarily those from the axon hillock and axons), and some come from non-spiking parts of the neuron surface.

Writing Ns_j for the spiking and Nns_j for the non-spiking part of neuron N_j we have

$$v_i^{\mathrm{spike}}(N_j, t) = \int\limits_{dA \in \mathrm{Ns}_j} I_{dA}(t) r(\vec{x_i}(dA)) dA \tag{4}$$

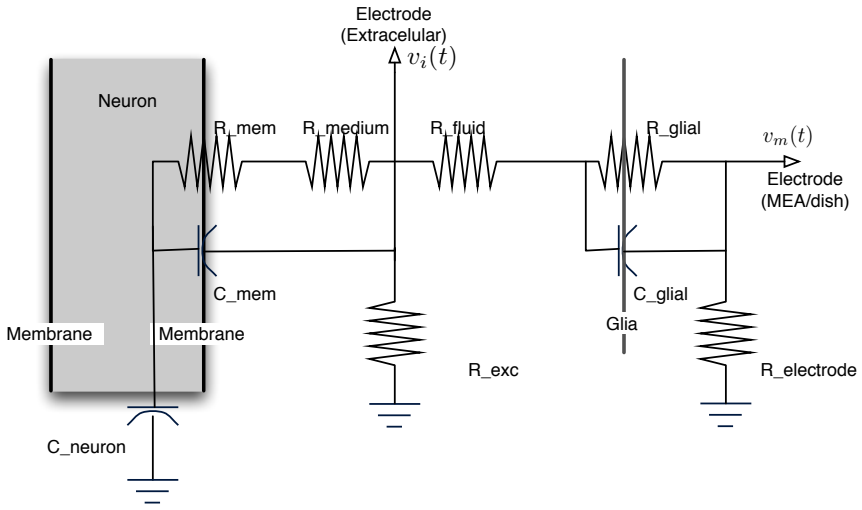

Figure 2. Equivalent circuit description for extracellular and dish based electrodes. The extracellular electrode is assumed to be near the neuron, but the dish electrode is assumed to have a layer of glia between it and the neural culture. There are a number of simplifications in this circuit: distributed resistances and capacitances have been lumped together, for example.

and

$$v_i^{\text{nonspike}}(N_j, t) = \int\limits_{dA \in \text{Nns}_j} I_{dA}(t) r(\vec{x}_i(dA)) dA \tag{5}$$

2.2 Action potentials

We can now consider $v_i^{\text{spike}}(N_j, t)$ due to a single spike at time T in neuron N_j. Assuming that "at time T" means that T is the time of the initiation of the spike at the axon hillock (i.e. the start of the self-reinforcing Na^+ inflow), $v_i^{\text{spike}}(N_j, t)$ from this spike will be 0 for $t < T$. We also assume that there is an upper bound on the duration of the effect of the spike at time T. The upswing of the spike is generated by runaway inflow of Na^+ ions, from the rapidly inactivating $I_{Na,t}$ channels, and the downswing by the outflow of K^+ ions from the I_K channels (Koch, 1999): these are the $I_{dA}(t)$ in equations 1 to 5. These charge and discharge the essentially capacitative intracellular (conducting) fluid of the neuron (which is largely insulated from the extracellular fluid by the insulating bilipid membrane). Thus, writing $V_{\text{spike}}(y, t)$ for the intracellular spike at location y (with respect to an external ground), and ignoring ohmic conduction within the neuron

$$V_{\text{spike}}(y, t) = \int dt \int\limits_{dA \in \text{nbhd}(y)} I_{dA}(t) dA / C_y \tag{6}$$

$$= \int dt \int\limits_{dA \in \mathrm{nbhd}(y)} (I^{\mathrm{Na}}_{dA}(t) + I^{\mathrm{K}}_{dA}(t))dA/C_y$$

where nbhd(y) is the membrane near y and C_y is the membrane capacitance of nbhd(y), so that

$$V'_{\mathrm{spike}}(y,t) = (I^{\mathrm{Na}}(y,t) + I^{\mathrm{K}}(y,t))/C_y \tag{7}$$

where $I^{\mathrm{Na}}(y,t)$ and $I^{\mathrm{K}}(y,t)$ are the ionic currents integrated over nbhd(y).

These ionic currents alter the extracellular potential, as described in equation 4. Thus

$$v_i^{\mathrm{spike}}(N_j,t,\mathrm{ion}) = \int\limits_{dA \in \mathrm{Ns}_j} (I^{\mathrm{Na}}(dA,t) + I^{\mathrm{K}}(dA,t))r(\vec{x}_i(dA)dA \tag{8}$$

Although we cannot actually incorporate equations 7 and 8 directly, it is clear that the extracellular potential at electrode i due to the ionic currents causing the spike is essentially the derivative of the intracellular spike weighted by the response function $r(\vec{x}_i)$.

In addition, there is also the electrical resistance and the capacitance of the membrane to take into account. The resistance of the membrane and the resistance between the extracellular fluid and the ground form a potential divider: in addition, the capacitance of the membrane and the resistance between the extracellular fluid and the ground act as a differentiator. Writing $v_i^{\mathrm{spike}}(N_j,t,\mathrm{mem})$ for the extracellular voltage from this source, we have

$$\begin{aligned} v_i^{\mathrm{spike}}(N_j,t,\mathrm{mem}) = & \frac{R_{\mathrm{exc}}}{R_{\mathrm{exc}} + R_{\mathrm{mem}} + R_{\mathrm{medium}}} V_{\mathrm{spike}}(t) \\ & + \frac{R_{\mathrm{exc}}}{R_{\mathrm{exc}} + R_{\mathrm{medium}}} C_{\mathrm{mem}} R_{\mathrm{exc}} V'_{\mathrm{mem}}(t) \end{aligned} \tag{9}$$

where $V'_{\mathrm{mem}}(t)$ is the derivative of the voltage across the membrane. The total potential at the extracellular electrode i from the spike at neuron N_j, $v_i^{\mathrm{spike}}(N_j,t) = v_i^{\mathrm{spike}}(N_j,t,\mathrm{ion}) + v_i^{\mathrm{spike}}(N_j,t,\mathrm{mem})$. This is therefore a mixture of the original spike, the differential of the spike, and a response weighted version of the differential of the spike. Since $R_{\mathrm{mem}} \gg R_{\mathrm{mem}} + R_{\mathrm{medium}}$, the contribution from the original spike will be small.

For an electrode some distance from neuron N_j in the intracellular fluid, the effect of the integration over the surface of the neuron will be to low-pass filter the signal (Struijk and Yoshida, 2004) because the spike is not generated at the same instant throughout the parts of the neuron that spike. In equation

8, $r(\vec{x}_i(dA))$ will decrease exponentially with distance due to diffusion: in equation 9 R_{medium} will increase linearly with distance. The precise effect on signal size from this is difficult to predict, but suggests that the contribution from the differential of the spike will decrease rather faster than linearly, at least for small distances from the spiking neuron to the electrode.

For a patch clamp electrode, for a small patch of membrane only, R_{exc} is replaced by a capacitor, so that equation 8 no longer holds, but instead $v_i^{\text{spike}}(N_j, t, \text{ion})$ is proportional to (but of opposite polarity from) $V_{\text{spike}}(t)$. In addition, V_{mem} and V'_{mem} are normally held at 0, and the currents involved in $\frac{R_{\text{exc}}}{R_{\text{exc}}+R_{\text{mem}}}V_{\text{spike}}(t)$ are relatively small, so that the ionic currents dominate.

For an electrode at the bottom of a culture dish, there is a further complication: glial cells are likely to form a (possibly incomplete) layer between the electrode and the neural culture. This layer may have a high resistance (R_{glial}), also acts as a capacitor (C_{glial}). However, in this case, we do not have ionic channels contributing to the potential at the electrode, so that only equation 9 is relevant. Writing $v_k^{\text{spike}}(N_j, t)$ for the voltage on electrode k at the bottom of the dish, we have

$$\begin{aligned} v_k^{\text{spike}}(N_j, t) = & \frac{R_{\text{electrode}}}{R_{\text{electrode}} + R_{\text{fluid}} + R_{\text{glial}}} v_i^{\text{spike}}(N_j, t) \\ & + C_{\text{glial}} R_{\text{electrode}} v_i'^{\text{spike}}(N_j, t) \end{aligned} \tag{10}$$

Of course, we do not have both electrodes i and k. In reality, $v_k^{\text{spike}}(N_j, t)$ results from the integration of $v_i^{\text{spike}}(N_j, t)$ over a volume of the nearby intracellular fluid. The primary effect of this is low-pass filtering.

What we actually receive at electrode k (whether extracellular or MEA based) is $s_k(t)$ which consists of $v_k^{\text{spike}}(N_j, t)$ from many different neurons N_j plus an additional noise signal, $n(t)$ from the receiving apparatus itself. Focussing on the signal from one neuron, N_j we can write this as

$$\begin{aligned} s_k(t) &= v_k(t) + n(t) \\ &= v_k(N_j, t) + \sum_{p \neq j} v_k(N_p, t) + n(t) \\ &= v_k^{\text{spike}}(N_j, t) + \sum_p v_i^{\text{nonspike}}(N_p, t) + \sum_{p \neq j} v_k^{\text{spike}}(N_p, t) + n(t) \end{aligned} \tag{11}$$

The first term is the "signal", and the other three are noise terms, in the sense that they do not originate from the spike at neuron j. Both the signal term and the noisy spiking term in equation 11 depend on the nature of the connection between the neurons and the electrode k, as discussed in equations 6 to 10. Part will be resistive, mediated by the ionic conduction of the medium,

part will be capacitative (and differentiating) due to the insulating membrane and the ion channels. Further, smoothing will have occurred. For MEA type electrodes, this will be compounded by insulating glial cells between the patch and the electrode causing a further mixture of resistive and capacitative (differentiating) coupling. Further, the potential will also depend on the nature of the transferrence of ionic current in the medium to electrical current in the electrode (not modelled here: (see Standen et al., 1987)).

The final result will be that a MEA electrode detects a mixture of $V_{\text{spike}}(t)$, $V'_{\text{spike}}(t)$ and $V''_{\text{spike}}(t)$, each smoothed to some extent. (We note that if there are other glial cells in the signal path, there may be further differentiation occurring as well.) For situations in which the electrode itself may be maneuvered, the value of $\vec{x}_i$ (in equation 4) can be reduced, improving the overall conductance between dA and the electrode. Further one might also attempt to place the electrode where the capacitative effects of glial cells are minimised (for example by shaping points on the electrodes, or by lowering the electrodes on to the culture). For patch clamping, the electrode is placed in electrolyte, and the electrolyte is directly attached to a patch of the membrane of the neuron of interest, so that $r(\vec{x}_i(dA))$ is essentially 0 and the connection primarily ionic for those dA inside the patch area.

The noise terms in equation 11 identify three components. The first (and probably smallest of these) arises from nonspiking events from nearby neurons. $I_{dA}(t)$ in these events is generally quite small, so that the contribution at the electrode is large only if $r(\vec{x}_i(dA))$ is large, which is likely to be the case only if dA is very close to the electrode, or if a patch is made to a nonspiking part of the electrode. Assuming that we are not using patch clamping, then this interference arises from nearby synaptic events, and non-axonic spikes (e.g. Ca^{++} spikes). The second noise term is likely to be the dominant term: this arises from spikes in other nearby neurons. In many situations, neurons are closely packed, so that if it has not been possible to place the electrode very close to the neuron of interest, noise from other neurons will be dominant. As with the signal term, the modes of transmission are as discussed earlier (and are likely to differ in relative strength for different neurons): one effect of this is that the detected spike shape is likely to differ for different nearby neurons (even if the intra-neuron spike shapes are identical), thus permitting spike sorting. The last noise term arises from extraneous electro-magnetic interference, and from the amplifiers used, and can be minimised by shielding and appropriate experimental design.

The distribution of the noise signal is likely to be quite different for each of the three sources of noise: for the first noise source, it is likely that these will be synaptic activity before and during spiking. For the second source, it is likely that nearby neurons receive similar input to the neuron of interest, so that they fire at similar times. Thus both of these noise sources will be correlated

to the signal of interest. The spike times from further away neurons are likely to be relatively independent of the neurons of interest. Only the last noise source is likely to be entirely uncorrelated.

3 Generating data for analysis

The main aim of this work is to enable the comparison of a number of different spike detection and sorting techniques. Without "ground truth" information, detailed comparison is impossible. Thus, in order to assist in these comparisons, we have produced a set of MATLAB functions to generate realistic data, using the analysis in section 2 to guide data generation. The functions have a number of variable parameters, enabling a wide range of data generation. In particular, we can generate data which has realistic signals from nearby neurons (the target neurons) and which has a large quantity of realistic noise (that is, realistic data from other neurons). It is possible to make the spiking of some of the other neurons correlated with target neurons, so that the signal from them is correlated with the signal from some of the target neurons. Other neurons can be spiking independently (independent neurons).

Overall, the data generation system has a number of phases: firstly, the spike times for the neurons of interest (target neurons) are generated, within some time interval. Spikes may be generated using either a Poisson or a Gaussian distribution. The mean inter-spike interval, and the degree of randomness of these spikes are variable. Once these spike times have been determined, we can generate spike times for other neurons (correlated neurons) each of whose spike trains are correlated with one of the target neurons. This is achieved by creating new spike times by allowing a (selectable) degree of jitter on the spike times of the target neuron. The software also allows generation of other sequences of spike times uncorrelated with the target spike times (independent neurons). We thus have one set of sequences of spike times, from the target neurons, plus two other sets of spike times, one correlated with the originals, and one not.

We use realistic spike shapes, (currently taken from the Hodgkin Huxley simulator HHSim (Touretzky et al., 2004), but they may be taken from elsewhere) to generate the intracellular potential for each of these spike trains. Where the inter-spike interval is less than the length of the spike shape, we join them smoothly, and in such a way that both reach their maximum potential. Minimum inter-spike intervals can be enforced. We then generate smoothed first and second differentials for all of these signals, and set all these signals and differentials to a normalised size. For each neural signal source (original, correlated and uncorrelated), we form a signal by linearly mixing the original intracellular signal and its smoothed differentials: the mixing parameters are

set by the user. These linearly mixed signals (characteristic of each spiking neuron) can then themselves be linearly mixed, allowing any required signal to noise ratio. Gaussian random noise (of selectable size) can be added at the end. This final signal can then be scaled to an appropriate range. In this way, we can generate a noisy signal similar to that which would be picked up by an electrode for which the actual timing of the spikes is known, and the precise form and extent of the noise can be adjusted. Further details of the noisy spike generation system (and MATLAB code) may be found in (Smith and Mtetwa, 2005).

4 An example

For this example, we choose to have four target neurons, seven correlated neurons, and five independent neurons. Two of the target neurons have a Poisson distribution, and the other two target neurons have a Gaussian distribution. The target neurons are closer than the others to the electrode. The seven correlated neurons are correlated with different target neurons. The relative strengths of the original, differentiated, and twice differentiated signals are shown in table 1. Equations 9 to 10 provide the justification for using such linear mixtures, but do not directly provide values for the actual relative strengths for these values. Since $R_{\text{mem}} \gg R_{\text{exc}}$, equation 9 suggests that the coefficient for the original signal (D0) should be small. Further, since $V_{\text{spike}}(t)$ changes very rapidly, $V'_{\text{mem}}(t)$ will be relatively large, suggesting that the coefficient of the first derivative should be larger. The extent of the coverage of the electrode, or of the path from the neuron to the electrode by glial cells is unknown, and may vary from neuron to neuron. Thus, we have varied the values for the coefficients for the first and second derivatives, D1 and D2, from neuron to neuron.

The relative location of the neurons is also shown in table 1: in the simulation, the overall strength of the signal from each neuron was set inversely proportional to the square of the distance from the electrode (but this is set by the experimentor, not directly in the code, so that a different relationship between distance and strength may be chosen). Although the intracellular spike shapes for the target neurons are identical, the different parameters for D0, D1, and D2 result in different signals being received at the electrode (see figure 3). The final signal received at the electrode is shown in figure 4.

The software can also be used to generate "spiky" background noise. To do this, the number of target neurons is set to zero, as is the number of correlated neurons. In the example in figure 5, the number of independent neurons was set to 10, and their parameters set so that the spike distributions were Gaussian, with mean inter-spike interval (ISI) 10ms, with a mean standard deviation

Table 1
Coefficients chosen for original (D0), differential (D1) and 2nd differential (D2) of signal. The location is in abstract units, relative to the electrode location of $(0, 0)$.

No	type	D0	D1	D2	location	
1	target	0.001	0.3	0.5	-1	-1.5
2	target	0.002	0.2	0.6	1.5	2
3	target	0.002	0.5	0.4	-1	2
4	target	0.002	0.8	0.1	-0.5	2
5	corr	0.002	0.5	0.2	2	10
6	corr	0.001	0.2	0.5	6	0
7	corr	0.002	0.4	0.6	5	-7
8	corr	0.001	0.3	0.7	-4	-7
9	corr	0.001	0.7	0.1	-7	-1
10	corr	0.003	0.25	0.45	-7	4
11	corr	0.003	0.4	0.2	-2	11
12	ind	0.003	0.3	0.7	8	5
13	ind	0.002	0.4	0.6	8	-5
14	ind	0.004	0.6	0.4	1	-10
15	ind	0.005	0.5	0.5	-5	-4
17	ind	0.002	0.75	0.3	-5	8

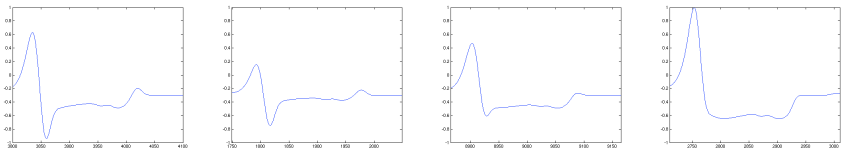

Figure 3. The shapes of the traces received at the electrode from a spike from each of the four target neurons (1-4 in table 1). Each graph shows 3 milliseconds.

of 1ms and minimum ISI of 1ms, with the original signal level set randomly between 0 and 0.003, and the contribution of the first and second derivative set randomly between 0 and 0.5. The spiky background noise and the distribution are shown in figure 5. For the spiky background noise produced by the spike trains generated here, the skewness of the distribution was 0.6, and the kurtosis was 4.16. In this case, the mean time between spikes is 0.53 ms, so that they will generally collide. Increasing the mean ISI to 1.4 ms leads to kurtosis of 6.41, and increasing the number of neurons to 50 (so that the mean time between spikes is 0.1 ms, much less than the actual length of a spike) decreases

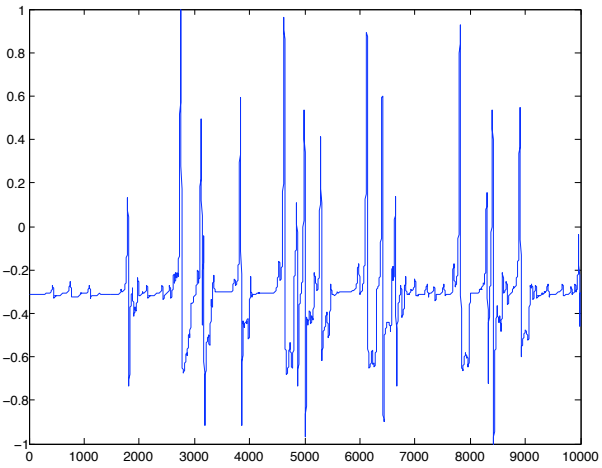

Figure 4. Signal received at the electrode, generated from coefficients in table 1. X axis is samples at 100,000 samples/second.

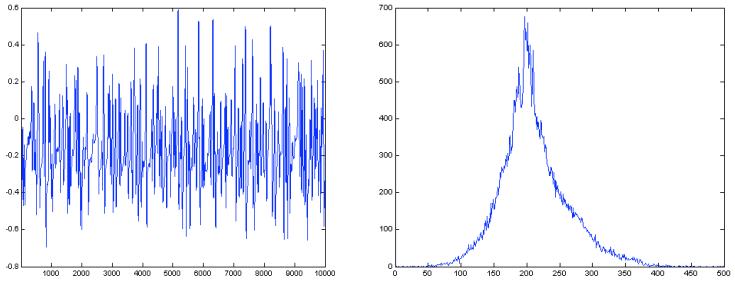

Figure 5. Spiky noise generated from 10 independent spike trains. Left shows 10,000 samples (0.1 seconds), and right shows distribution of the values.

the kurtosis to 3.19. Thus, the number of neurons and other parameters can be chosen to provide the appropriate form of spiky background noise.

5 Conclusions and further work

We have presented a biophysical model for the transfer of electrical signals from neural spikes to an electrode. In this model, we have considered the electrode to be a charge sensor: that is a very high impedance input device. From the analysis, we have produced a piece of software in MATLAB which can generate realistic signals for which the locations (and shapes) of the underlying spike trains are known. We believe that this software can generate synthetic noisy signals which can be of use in assessing the effectiveness of algorithms for spike detection and sorting. The software may be used either directly, or as a mechanism for generating realistic non-Gaussian background noise.

The software could be extended to generate more than one electrode signal. Where they are so far apart that they are independent (which is normally the case in current MEAs), this is unnecessary (the software can simply be run more than once). However, if, for example, the electrodes were closely spaced tetrodes, we could use their precise positioning, and determine the precise parameters for the neurons for each electrode, and thus produce a set of synthetic spike trains, one for each electrode. Another possible extension would be to allow the modelling of bursting neurons.

6 Acknowledgements

Nhamo Mtetwa was funded by the UK EPSRC throughout this research. We acknowledge useful discussions with Adam Curtis, Bruce Graham, Douglas McLean, Nikki MacLeod and Alan Murray.

References

Atiya, A., 1992. Recognition of multiunit neural signals. IEEE Transactions on Biomedical Engineering 39, 723–729.

Bower, J., Beeman, D., 1998. The book of GENESIS, 2nd Edition. Springer Verlag.

Chandra, R., Optican, L., 1997. Detection, classification and superposition resolution of action potentials in multiunit single channel recordings by an on-line real-time neural network. IEEE Transactions on Biomedical Engineering 44, 403–412.

Koch, C., 1999. Biophysics of Computation. Oxford.

Lewicki, M., 1998. A review of methods for spike sorting: the detection and classification of neural potentials. Network: Comput. Neural Syst. 9, R53–R78.

Mamlouk, A., Sharp, H., Menne, K., Hoffmann, U., Martinetz, T., 2005. Unsupervised spike sorting with ICA and its evaluation using GENESIS algorithms. Neurocomputing 65-66, 275–282.

Menne, K., Folkers, A., Malina, T., Maex, R., Hoffmann, U., 2002. Test of spike sorting algorithms on the basis of simulated network data. Neurocomputing 44-46, 1119–1126.

Menne, K., Malina, T., Hoffmann, U., 2005. Test of spike sorting algorithms on the basis of simulated network data. In: Polani, D., Kim, J., Martinetz, T. (Eds.), Fifth German Workshop on Artificial Life:Abstracting and Synthesizing the Principle of Living Systems. IOS Press.

Nakatani, H., Watanabe, T., Hoshimiya, N., 2001. Detection of nerve action

potentials under low signal-to-noise ratio condition. IEEE Transactions on Biomedical Engineering 48, 845–849.

Quiroga, R. Q., Nadasdy, Z., Ben-Shaul, Y., 2004. Unsupervised spike detection and sorting with wavelets and superparamagnetic clustering. Neural Computation 16, 1661–1687.

Smith, L., Mtetwa, N., 2005. Manual for the noisy spike generator matlab software. at URL http://www.cs.stir.ac.uk/~lss/noisyspikes/.

Standen, N. B., Gray, P. T. A., Whitaker, M. J., 1987. Microelectrode Techniques: the Plymouth Workshop Handbook. The Company of Biologists, Cambridge.

Struijk, J. J., Yoshida, K., 2004. Volume conduction. at URL www.smi.hst.aau.dk/npig/seminar/2004/0312JJSVolumeConduction.pdf.

Touretzky, D., Albert, M., Daw, N., Ladsariya, A., 2004. HHsim: Graphical hodgkin-huxley simulator. at URL http://www.cs.cmu.edu/ dst/HHsim/.

Wood, F., Black, M., Vargas-Irwin, C., Fellows, M., Donoghue, J., 2004. On the variability of manual spike sorting. IEEE Transactions on Biomedical Engineering 51, 912–918.

Zhang, P.-M., Wu, J.-Y., Zhou, Y., Liang, P.-L., Yuan, J.-Q., 2004. Spike sorting based on automatic template reconstruction with a partial solution to the overlapping problem. Journal of Neuroscience Methods 135, 55–65.